Coriolis coupling as a source of non-RRKM effects in ozone molecule: Lifetime statistics of vibrationally excited ozone molecules

M. Kryvohuz and R. A. Marcus[a)]
Noyes Laboratories, 127-72, California Institute of Technology, Pasadena, California 91125, USA

(Received 27 October 2009; accepted 27 April 2010; published online 8 June 2010)

A theory that describes the non-RRKM (non-Rice-Ramsperger-Kassel-Marcus) effects in the lifetime statistics of activated ozone molecules is derived. The non-RRKM effects are shown to originate due to the diffusive energy exchange between vibrational and rotational degrees of freedom in ozone molecule. The lifetime statistics is found to be intramolecular diffusion controlled at long times. The theoretical results are in good agreement with the direct MD simulations of lifetime statistics. © *2010 American Institute of Physics*. [doi:10.1063/1.3430514]

I. INTRODUCTION

In the previous paper[1] hereafter referred as Part I, we have shown that the intramolecular energy exchange between the rotational and vibrational degrees of freedom in the vibrationally excited triatomic molecule has a diffusive behavior. For ozone, this diffusion process is fast enough to violate the assumption of adiabaticity of rotational degrees of freedom, yet slow enough to consider these degrees of freedom active.[1,2] We therefore expect some non-RRKM (non-Rice-Ramsperger-Kassel-Marcus) effects in the process of ozone formation. An explicit stochastic differential equation that governs this intramolecular diffusion was derived in Part I. In the present paper, we use stochastic analysis to study analytically the non-RRKM effects caused by diffusive energy exchange between the rotational and vibrational degrees of freedom in ozone.

Recent classical molecular dynamics (MD) simulations[3,4] revealed non-RRKM effects in the distribution of lifetimes of activated ozone molecules. The distribution functions that were obtained consisted of multiple exponential decays, some of them had a slow long-time tails while the others did not have such tails. In the present paper, we show that the observed nonstatistical behavior of lifetime distributions is a result of diffusive Coriolis energy exchange between the rotational and vibrational degrees of freedom. Using the Fokker–Planck approach, we derive an analytical expression for the lifetime distribution functions obtained in numerical simulations.[3,4]

The paper is organized as follows. In Sec. II a differential equation for the intramolecular probability distribution density is derived. In Sec. III an analytical expression for the dissociation rate appearing in this differential equation is obtained. In Sec. IV the resulting differential equation is solved numerically and is compared with the results of MD simulations. In Sec. V an approximate analytical solution of this equation is provided and the analytical expression for the lifetime distribution function is derived. Results are summarized and discussed in Sec. VI.

[a)]Electronic mail: ram@caltech.edu.

II. DIFFERENTIAL EQUATION FOR THE DISTRIBUTION DENSITY

In Part I we showed that the dynamics of the K-projection of the total rotational angular momentum $\mathbf{J}$ of vibrationally excited ozone molecule during its lifetime can be effectively described by a simple stochastic equation

$$\frac{dK}{dt} = -\sqrt{2D_c}K + \sqrt{J^2 - K^2}\sqrt{D_c}\xi(t), \tag{1}$$

where $\xi(t)$ is a delta-correlated noise $\langle \xi(t)\xi(0)\rangle = 2\delta(t)$ and $D_c(K)$ is a function of K, which for the ozone molecule $^{48}O_3$ was found in Part I from numerical analysis of the rate of K-diffusion to be $D_c(e_{\mathrm{vib}}(K)) = 0.000\,04 + 0.0015\exp(-15(e_{\mathrm{vib}} - 0.05)^2)$ ps^{-1}, where $e_{\mathrm{vib}} \equiv E_{\mathrm{vib}} - E_{\mathrm{diss}} = E - E_{\mathrm{rot}} - E_{\mathrm{diss}}$ is an excess vibrational energy in eV for a vibrationally excited ozone molecule with total energy E and dissociation barrier E_{diss}.

We consider a vibrationally excited ozone molecule with the total energy E, which is greater than the dissociation barrier E_{diss}. We assume that its total rotational angular momentum J is such that the total vibrational energy $E_{\mathrm{vib}} = E - E_{\mathrm{rot}}$ can be less than E_{diss}. The rotational energy of ozone molecule can be written as[1]

$$E_{\mathrm{rot}}(K) = \frac{J^2}{2\sqrt{\langle I_2\rangle\langle I_3\rangle}} + \left(\frac{1}{2\langle I_1\rangle} - \frac{1}{2\sqrt{\langle I_2\rangle\langle I_3\rangle}}\right)K^2, \tag{2}$$

where $\langle I_i\rangle$ are the average principal moments of inertia and K may take values from $-J$ to J. Let us denote the value of K that corresponds to the condition $E - E_{\mathrm{rot}} = E_{\mathrm{diss}}$ by

$$K_{\max} \equiv \sqrt{\frac{2(E - E_{\mathrm{diss}}) - J^2/\sqrt{\langle I_2\rangle\langle I_3\rangle}}{(1/\langle I_1\rangle) - (1/\sqrt{\langle I_2\rangle\langle I_3\rangle})}}. \tag{3}$$

For the values of K such that $|K| > K_{\max}$, the vibrational energy of ozone molecule is less than the dissociation barrier E_{diss} and so the ozone molecule is not able to dissociate (these vibrational energies correspond to closed states (or channels) in Ref. 5). For the values of K such that $|K| < K_{\max}$, the vibrational energy of ozone molecule is greater than the dissociation barrier and therefore ozone molecule can easily dissociate (these vibrational energies correspond

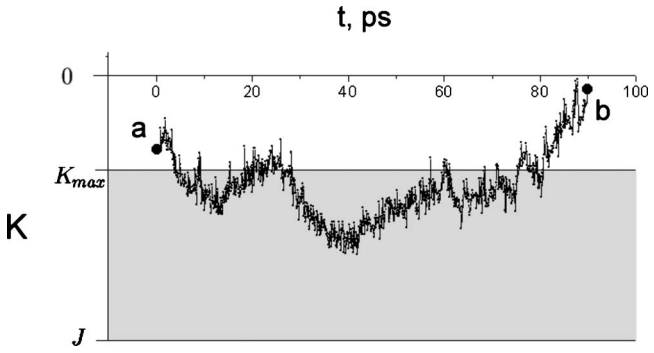

FIG. 1. An effective diffusion of K-projection of rotational angular momentum in ozone molecule. The figure represents a single trajectory of $K(t)$ from the MD simulation of a molecule of ozone. Point (a) corresponds to the formation of ozone molecule, point (b) corresponds to the dissociation of ozone molecule. The dark region corresponds to the energies at which ozone molecule cannot dissociate (closed states); the white region corresponds to open states.

to open states in Ref. 5), as in Fig. 1. One can see that the possibility of ozone molecule to dissociate is controlled by the value of K, while the latter is controlled by the diffusion process in Eq. (1). Therefore the lifetimes of an excited ozone molecule is controlled by the process of diffusion (1), which means highly nonstatistical (non-Poissonian) distribution of lifetimes of excited ozone molecules.

For the values of J and E such that $E-E_{\mathrm{rot}}^{\max}>E_{\mathrm{diss}}$ the vibrational energy is always greater than the dissociation limit and $K_{\max}=J$. In this case the effect of a Coriolis driven intramolecular energy diffusion is small since the dissociation rate of vibrationally excited ozone is much faster (as shown in the next section) than the rate of vibrational-rotational energy exchange. For the same reason these values of E and J do not result in the slow long time "tails" of lifetime distribution functions of vibrationally excited ozone molecules in the numerical MD simulations performed in Refs. 3 and 4. To illustrate the effect of rotations hereafter in this paper we consider only the values of E and J that allow $E-E_{\mathrm{rot}}^{\max}<E_{\mathrm{diss}}$ and $K_{\max}<J$.

In the present analysis, we do not consider the centrifugal effect on the dissociation barrier and hereafter assume E_{diss} to be a constant independent of J. Centrifugal effect is not essential in our model for the following reason. The ratio of the maximum I_3 and the minimum I_1 moments of inertia in an ozone molecule with C_{2v} symmetry is 10 to 1, as noted in Part I. The maximal decrease of dissociation barrier of the O–O bond of length r_0 due to the centrifugal effect is achieved at zero value of the K-component of the total angular momentum $\mathbf{J}$ and can be estimated as $\Delta E_{cf}=m\Omega^2 r_0^2/2=m(J/I_3)^2(I_3/2m)/2=J^2/4I_3$. On the other hand, the maximum rotational energy of ozone for a given J is achieved at $K=J$ and equals $E_{\mathrm{rot}}^{\max}=J^2/2I_1$, which is 20 times greater than ΔE_{cf}. Thus, in the process of interest, diffusion of K toward its large values, the centrifugal effect is expected to contribute only up to 10%. Taken into consideration the fact that the fluctuation of inertia moments due to the large amplitude vibration at energies near the dissociation limit is about 20% (for I_3) to 50% (for I_1), as noted in Part I, the centrifugal effect can be neglected for the present purpose.

To treat quantitatively the diffusion Eq. (1) we utilize a Fokker–Planck equation technique. We introduce a probability distribution density $\rho(K,t)$ that describes the probability of K to take values between K' and $K'+dK$ in a time interval $(t,t+dt)$. Clearly, $\rho(K,t)$ should be finite at the boundaries $K=\pm J$ and be symmetric on the interval $(-J,J)$ with respect to $K=0$, which implies the boundary condition $\partial\rho(0,t)/\partial K=0$. The Fokker-Planck equation that corresponds to the diffusion Eq. (1) is[6]

$$\frac{\partial\rho(K,t)}{\partial t}=-\frac{\partial}{\partial K}\left(\frac{1}{2}\frac{\partial D(K)}{\partial K}-\sqrt{2}KD_c\right)\rho(K,t)+\frac{\partial^2}{\partial K^2}D(K)\rho(K,t), \tag{4}$$

where $D(K)\equiv(J^2-K^2)D_c(K)$. Equation (4) states that the probability density can be changed only by the process of diffusion. Yet, we know that on the K interval $(-K_{\max},K_{\max})$ the ozone molecule dissociates and thus the probability density on this interval also decreases with the rate of dissociation r, which can be a function of K. Thus, the complete differential equation for the probability density is

$$\frac{\partial\rho(K,t)}{\partial t}=-\frac{\partial}{\partial K}\left(\frac{1}{2}\frac{\partial D(K)}{\partial K}-\sqrt{2}KD_c\right)\rho(K,t)+\frac{\partial^2}{\partial K^2}D(K)\rho(K,t)-r(K)\rho(K,t) \tag{5}$$

with $r(K)=0$ for $|K|>K_{\max}$ and initial distribution density $\rho(K,0)=\rho_0(K)$. For the present model we can assume that no value of K is preferred over the others at time $t=0$ (at the moment of formation of an excited ozone molecule), thus the initial distribution density can be taken as a uniform step function

$$\rho_0(K)=\begin{cases}1/(2K_{\max}), & |K|<K_{\max}\\ 0, & K_{\max}<|K|<J.\end{cases} \tag{6}$$

In the following sections, we provide a solution to the Eq. (5) and then use it to derive the lifetime distribution function of excited ozone molecules.

III. THE RATE OF DISSOCIATION $r(K)$

The diffusive nature of $K(t)$ in Eq. (1) suggests that we can keep K as adiabatic parameter in calculation of the dissociation rate $r(K)$. The dissociation rate r is then a function of the total vibrational energy E_{vib} only and one should write $r(E_{\mathrm{vib}}(K))$ instead. To calculate $r(E_{\mathrm{vib}})$, one can apply RRKM theory that includes *only* vibrational degrees of freedom. For the purposes of present analysis, the direct numerical computation of $r(E)$ is sufficient. For this purpose, we perform microcanonical sampling[7] of *nonrotating* ozone molecules with a fixed total energy $E>E_{\mathrm{diss}}$, record statistics of their lifetimes and obtain $r(E)$ as a slope of Poisson distribution in log-scale, see Figs. 2(a) and 2(b). The details of the numerical simulations were described in "Numerical simulations" section in Part I. As expected, the distribution of lifetimes of nonrotating ozone molecules is purely statistical and does not show any non-RRKM behavior. It was shown in Part I

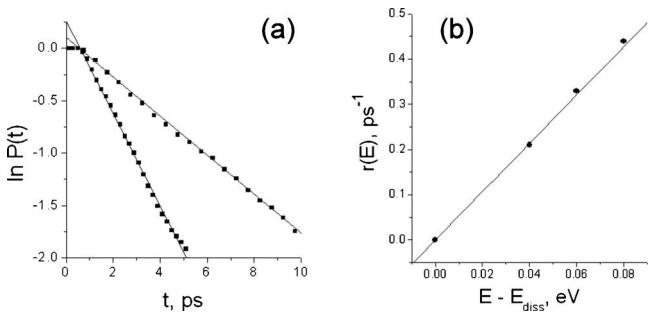

FIG. 2. Dissociation rate $r(E)$ of non-rotating ozone molecules as a function of excess energy above the dissociation barrier. Part (a) presents lifetime statistics $P(t)$ for the energies $E=E_{\mathrm{diss}}+0.04$ eV (top line) and $E=E_{\mathrm{diss}}+0.08$ eV (bottom line). Part (b) represents the rates $r(E)$ as a function of excess energy on the interval from 0 to 0.08 eV.

that the non-RRKM effects appear only if rotation is present. The best fitted line to the numerical results in Fig. 2(b) is $r(E_{\mathrm{vib}})=k_r(E_{\mathrm{vib}}-E_{\mathrm{diss}})$ ps^{-1}, where $k_r=5.2$ eV^{-1} ps^{-1}. We therefore finally obtain

$$r(K) \equiv r(E_{\mathrm{vib}}(K)) = k_r(E - E_{\mathrm{diss}} - E_{\mathrm{rot}}(K)) = c_1 - c_2K^2, \quad |K| < K_{\max}, \tag{7}$$

where $c_1=k_r(E-E_{\mathrm{diss}}-(J^2/2\sqrt{\langle I_2\rangle\langle I_3\rangle}))$ and $c_2=k_r[(1/2\langle I_1\rangle)-(1/2\sqrt{\langle I_2\rangle\langle I_3\rangle})]$ are constants for given total energy E and angular momentum J.

MD simulations[3,4] also observed another non-RRKM effect during the first two picoseconds of the formation of vibrationally excited ozone molecule in $O+O_2$ collision. This 2 ps time is the time that is required for the vibrational energy initially localized in the O–O bond of ozone that just formed to be redistributed among other vibrational degrees of freedom. In terms of the present model of diffusive energy exchange between vibrational and rotational degrees of freedom, this 2 ps is the time that is required for vibrational degrees of freedom to reach ergodicity regime from the initially localized vibration, which allows then to consider vibrational chaos as a random noise to rotations. Vibrational chaos is the key feature of the present model and in both the present and the previous papers is assumed to have been established. The non-RRKM effect of initial vibrational energy redistribution observed in Refs. 3 and 4 is thus not important for our model and can be disregarded. In addition, the non-RRKM effect mentioned above is observed only for the particular method of preparation of the vibrationally excited ozone molecule, i.e., by an $O+O_2$ collision. If the vibrationally excited ozone molecule is prepared from microcanonical sampling with random distribution of energies between *all* vibrational degrees of freedom, such as done in the numerical simulations of the present chapter, the above mentioned non-RRKM effect would not be expected to be found.

IV. SOLUTION FOR $\rho(K,t)$

Since the solution of Eq. (5) is symmetrical with respect to $K=0$ we solve this equation on the interval $K\in[0,J]$ with the initial distribution density $\rho(K,0)=2\rho_0(K), K>0$. The differential Eq. (5) can be greatly simplified after the change of variables from K to y,

$$y = y(K) = \int_0^K \frac{dK'}{\sqrt{D(K')}}. \tag{8}$$

The derivatives and distribution density appearing in Eq. (5) transform as[6]

$$\left(\frac{\partial}{\partial t}\right)_K = \frac{1}{\mathcal{J}}\left(\frac{\partial}{\partial t}\right)_y \mathcal{J},$$

$$\frac{\partial}{\partial K} = \frac{1}{\mathcal{J}}\frac{\partial}{\partial y}, \tag{9}$$

$$\frac{\partial^2}{\partial K^2} = \frac{1}{\mathcal{J}}\frac{\partial^2}{\partial y^2}\frac{1}{\mathcal{J}} + \frac{1}{\mathcal{J}}\frac{\partial}{\partial y}\frac{\partial \mathcal{J}}{\partial K}\frac{1}{\mathcal{J}},$$

$$\tilde{\rho}(y,t) = \mathcal{J}\rho(K,t),$$

where $\mathcal{J}=\sqrt{D(K)}$ is the Jacobian of transformation. Using Eqs. (8) and (10) in Eq. (5) we obtain a simplified differential equation for the new distribution density $\tilde{\rho}(y,t)$

$$\frac{\partial \tilde{\rho}}{\partial t} = \frac{\partial}{\partial y}\left(\frac{\sqrt{2}K(y)D_c}{\mathcal{J}(y)}\right)\tilde{\rho} + \frac{\partial^2 \tilde{\rho}}{\partial y^2} - r(K(y))\tilde{\rho} \tag{10}$$

with the boundary condition $\partial\tilde{\rho}(0,t)/\partial y=0$, zero probability flux at $y=y(J)$, i.e., $((\sqrt{2}K(y)D_c)/\mathcal{J}(y))\tilde{\rho}+\partial\tilde{\rho}/\partial y=0$ and initial distribution density $\tilde{\rho}_0(y,0)=2\sqrt{D(K)}\rho_0(K(y)), y>0$. Equation (10) is now readily solved numerically. Before doing so we derive the expression for the lifetime statistics that we are interested in. The distribution of lifetimes of the vibrationally excited ozone molecules is given by the expression for the first exit times[8]

$$p(t) = -\int_0^J \frac{\partial \rho(K,t)}{\partial t} dK. \tag{11}$$

If one is interested in the integrated lifetime statistics $P(t)=\int_t^\infty p(t')dt'$, the survival probability, which was used, for instance, in Refs. 3 and 4 then its expression is given by

$$P(t) = \int_0^J \rho(K,t)dK = \int_0^{y(J)} \tilde{\rho}(y,t)dy. \tag{12}$$

Clearly, $P(0)=1$. Results of the numerical solution of the second order partial differential Eq. (10) are shown in Fig. 3. One can see that there is good agreement of the theoretical solution and numerical results taken from Refs. 3 and 4. We want to emphasize that the lifetime statistics in Eq. (12) and the one calculated numerically in Refs. 3 and 4 is the statistics of self-dissociation times of isolated vibrationally excited molecules. If the collisions with other molecules are present, then the total lifetime statistics is the convolution of the self-dissociation probability and the probability of collision.[9]

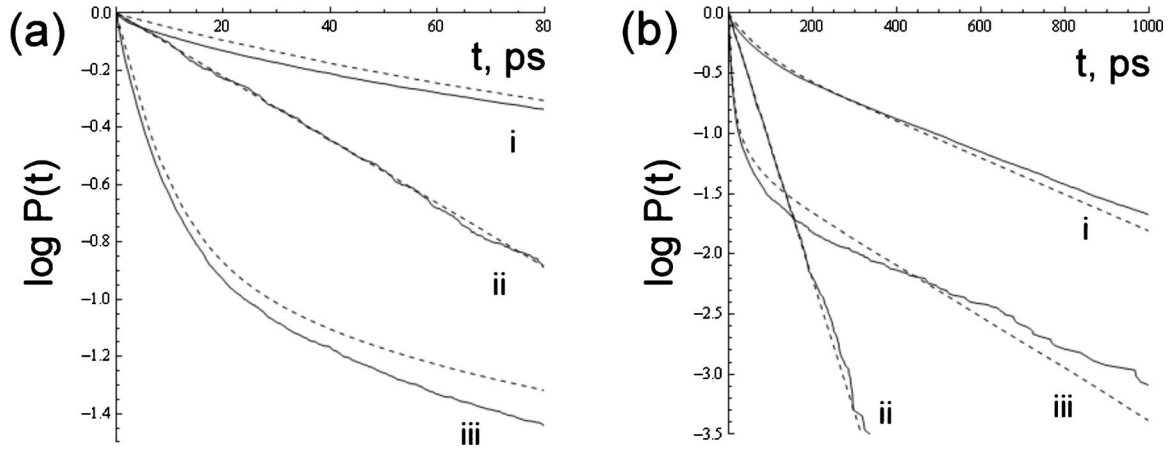

FIG. 3. Lifetime statistics $P(t)$ of excited ozone molecules. Solid lines are the results of MD simulations taken from Refs. 3 and 4. Dashed lines are the corresponding theoretical results obtained from solution of the differential Eq. (10). Curves (i) represent results for the total energy $E=E_{\text{diss}}+0.2\ kT$ and $J=5.6\hbar$; curves (ii) represent results for $E=E_{\text{diss}}+0.2\ kT$ and $J=0$; curves (iii) represent results for $E=E_{\text{diss}}+3\ kT$ and $J=22\hbar$, where $kT=0.025$ eV is room temperature. (a) represents the time interval from 0 to 80 ps; (b) represents the time interval from 0 to 1000 ps.

V. APPROXIMATE ANALYTICAL SOLUTION OF EQ. (10)

Equation (10) can be solved analytically with some degree of approximation. First, we disregard weak dependence of D_c on K and assume that D_c is a constant. In this case we easily find the analytical form of the parameters defined in the previous section,

$$y(K)=\frac{1}{\sqrt{D_c}}\arcsin\left(\frac{K}{J}\right),$$
$$\mathcal{J}(y)=\sqrt{D_c}J\cos(\sqrt{D_c}y). \tag{13}$$

Introducing new variable $x\equiv\sqrt{D_c}y$, with x defined on the interval $(-\pi/2,\pi/2)$, the Fokker–Planck Eq. (10) simplifies to

$$\frac{\partial\tilde{\rho}}{\partial t}=\sqrt{2}D_c\frac{\partial}{\partial x}\tan(x)\tilde{\rho}+D_c\frac{\partial^2\tilde{\rho}}{\partial x^2}-r(x)\tilde{\rho}, \tag{14}$$

with

$$r(x)=\begin{cases}c_1-c_2J^2\sin^2 x, & |\sin x|<\dfrac{1}{J}\sqrt{\dfrac{c_1}{c_2}},\\ 0, & |\sin x|\geq\dfrac{1}{J}\sqrt{\dfrac{c_1}{c_2}},\end{cases} \tag{15}$$

initial distribution density

$$\tilde{\rho}_0(x)=\begin{cases}\dfrac{J}{2}\sqrt{\dfrac{c_2}{c_1}}\cos x, & |\sin x|<\dfrac{1}{J}\sqrt{\dfrac{c_1}{c_2}},\\ 0, & |\sin x|\geq\dfrac{1}{J}\sqrt{\dfrac{c_1}{c_2}},\end{cases} \tag{16}$$

and boundary conditions

$$\frac{\partial\tilde{\rho}(0,t)}{\partial x}=0, \tag{17a}$$

$$\left(\sqrt{2}\tan x+\frac{\partial}{\partial x}\right)\tilde{\rho}|_{x=\pi/2}=0, \tag{17b}$$

which correspond to the requirement of the symmetry of the distribution density with respect to $x=0$ and the restriction of zero probability flux at $x=\pi/2$, respectively. One can notice the divergence of $\tan(x)$ in the boundary condition (17b) at $x=\pi/2$, which also results in zero probability density at $x=\pi/2$, i.e., $\tilde{\rho}(\pi/2,t)=0$, in addition to zero probability flux at the boundary.[6]

In the following two subsections, we obtain eigenfunctions $\tilde{\varphi}_n(x)$ and eigenvalues $\tilde{\varepsilon}_n$ of the diffusion Eq. (14). One can bypass the mathematical derivations of subsections A and B, if one is mainly interested in the final results and proceed directly to subsection C, where the results are presented.

A. The case of $r(x)=0$

First, we note that in the absence of dissociation rate $r(x)$, i.e., in case of total energies of ozone molecules lower than the dissociation threshold, the Fokker–Planck Eq. (14)

$$\frac{\partial\tilde{\rho}}{\partial t}=\boldsymbol{L}_{\text{FP}}\tilde{\rho}, \tag{18}$$

with the Fokker–Planck operator $\boldsymbol{L}_{\text{FP}}$

$$\boldsymbol{L}_{\text{FP}}\equiv D_c\frac{\partial}{\partial x}\left(\sqrt{2}\tan x+\frac{\partial}{\partial x}\right), \tag{19}$$

has a *stationary* solution

$$\tilde{\rho}_{st}(x)=N\cos^{\sqrt{2}}(x), \tag{20}$$

where N is a normalization constant. Representing the stationary solution in the form $\tilde{\rho}_{st}(x)=N\exp(-\Phi(x))$, we define a function $\Phi(x)$, which is necessary for further discussion

$$\Phi(x)=-\sqrt{2}\ln(\cos x). \tag{21}$$

In particular, the probability flux current $S(x,t)$ can now be expressed as[6]

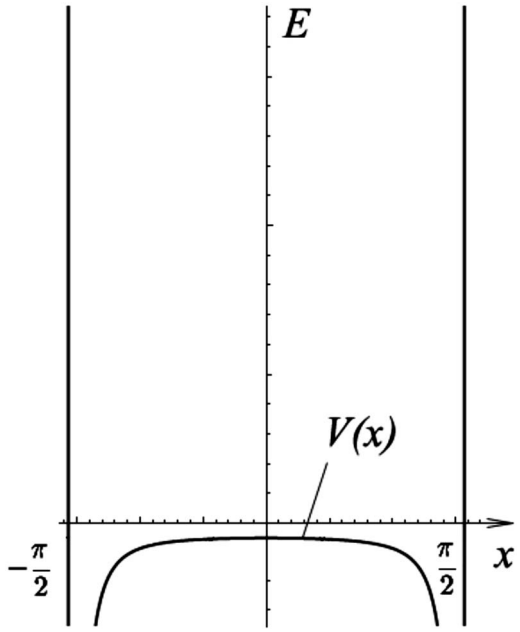

FIG. 4. Schrodinger potential $V(x)$ for the operator $\mathbf{L}$ in Eq. (24).

$$S(x,t) = -D_c\left(\Phi'(x) + \frac{\partial}{\partial x}\right)\tilde{\rho}(x,t). \tag{22}$$

To find the eigenfunctions and the eigenvalues of the non-Hermitian operator $\boldsymbol{L}_{\mathrm{FP}}$ it is convenient to consider a transformed Fokker–Planck Hermitian operator[6]

$$\boldsymbol{L} = e^{\Phi/2}\boldsymbol{L}_{\mathrm{FP}}e^{-\Phi/2}. \tag{23}$$

Both operators $\boldsymbol{L}_{\mathrm{FP}}$ and $\boldsymbol{L}$ have the same eigenvalues ε_n and their corresponding eigenfunctions φ_n and ψ_n, respectively, are related as $\psi_n(x)=\exp(\Phi(x)/2)\varphi_n(x)$.[6] Transformation (23) transforms operator $\boldsymbol{L}_{\mathrm{FP}}$ into the form similar to the negative single-particle Hamilton operator in quantum mechanics,[6] i.e.,

$$\boldsymbol{L} = D_c\frac{\partial^2}{\partial x^2} - V(x) \tag{24}$$

with

$$V(x) = \frac{D_c}{4}(\Phi'(x)^2 - 2\Phi''(x)), \tag{25}$$

thus eigenfunctions $\psi_n(x)$ and eigenvalues ε_n of the operator $\boldsymbol{L}$ are the solutions of the stationary Schrodinger equation of a particle in the potential $V(x)=D_c(\sin^2 x-\sqrt{2})/2\cos^2 x$.

We need to add a few comments on the form of the potential $V(x)$. It is clear that the function $(\sin^2 x-\sqrt{2})/2\cos^2 x$ has second derivative that is always negative, i.e., the latter function does not resemble a potential well but instead a hill, as in Fig. 4. However, boundary conditions of zero flux current at $x=\pm\pi/2$ in the Fokker–Planck Eq. (18) according to Eq. (22) give $D_c(\Phi'(x)+(\partial/(\partial x)))\tilde{\rho}(x,t)|_{x\to\pi/2}=0$. Representing $\tilde{\rho}(x,t)$ in the form $\tilde{\rho}(x,t)=\varphi(x)\exp(-\varepsilon t)$ we get the boundary conditions for eigenfunctions $\varphi_n(x)$: $D_c(\Phi'(x)+(\partial/(\partial x)))\varphi_n(x)|_{x\to\pi/2}=0$, which after integration in the vicinity of $x=\pi/2$ gives the behavior of $\varphi_n(x)$ at the boundary, i.e.,

$$\lim_{x\to\pi/2}\varphi_n(x) = C_n\lim_{x\to\pi/2}e^{-\Phi(x)} = C_n'\lim_{x\to\pi/2}\cos^{\sqrt{2}}x = 0, \tag{26}$$

The boundary condition for the eigenfunctions $\psi_n(x)$ of the operator $\boldsymbol{L}$ is therefore

$$\begin{aligned}\lim_{x\to\pi/2}\psi_n(x) &= \lim_{x\to\pi/2}e^{\Phi(x)/2}\varphi_n(x)\\ &= C_n\lim_{x\to\pi/2}e^{-\Phi(x)/2}\\ &= C_n'\lim_{x\to\pi/2}\cos^{1/\sqrt{2}}x = 0.\end{aligned} \tag{27}$$

Therefore, $x=\pi/2$ corresponds to the nonpenetrable wall at which all eigenfunctions $\psi_n(x)$ become zero (the same is clearly true for $x=-\pi/2$). Thus the Schrodinger potential that corresponds to the Hamiltonian (24) is the one shown in Fig. 4 and has a nontrivial form of an infinite potential well with double divergence at the boundaries $V(x\to\pm\pi/2)\to-\infty$ and $V(x=\pm\pi/2)=+\infty$. By direct substitution into Eq. (24) one can easily check that $\psi_0=\exp(\Phi(x)/2)\tilde{\rho}_{st}(x)$ is the ground state in this potential with the corresponding eigenvalue $\varepsilon_0=0$ (all other eigenvalues ε_n are positive, as proved in Ref. 6).

B. The case of $r(x)\neq 0$

The case $r(x)\neq 0$ corresponds to vibrationally activated ozone molecules with total energy above the dissociation threshold, which we are interested in. Using the definitions of the previous subsection, Eq. (14) reads

$$\frac{\partial\tilde{\rho}}{\partial t} = (\boldsymbol{L}_{\mathrm{FP}} - r(x))\tilde{\rho}. \tag{28}$$

The transformation $\exp(\Phi(x)/2)(\boldsymbol{L}_{\mathrm{FP}}-r(x))\exp(-\Phi(x)/2)$, with $\Phi(x)$ from Eq. (21), transforms a non-Hermitian operator $\tilde{\boldsymbol{L}}_{\mathrm{FP}}\equiv\boldsymbol{L}_{\mathrm{FP}}-r(x)$ into a Hermitian operator $\tilde{\boldsymbol{L}}\equiv\exp(\Phi(x)/2)\tilde{\boldsymbol{L}}_{\mathrm{FP}}\exp(-\Phi(x)/2)$, as seen in Appendix A, given explicitly by

$$\tilde{\boldsymbol{L}} = D_c\frac{\partial^2}{\partial x^2} - (V(x)+r(x)), \tag{29}$$

where $V(x)$ is the same function as in the previous subsection. The Schrodinger potential $(V(x)+r(x))$ is shown in Fig. 5(a). It follows from Appendix A that the operators $\tilde{\boldsymbol{L}}_{\mathrm{FP}}$ and $\tilde{\boldsymbol{L}}$ have the same eigenvalues $\tilde{\varepsilon}_n$ and their eigenfunctions $\tilde{\varphi}_n$ and $\tilde{\psi}_n$, respectively, are related by $\tilde{\psi}_n(x)=\exp(\Phi(x)/2)\tilde{\varphi}_n(x)$. The boundary conditions for $\tilde{\psi}_n(x)$ are the same as in Eq. (27). The appearance of the barrier $r(x)$ in addition to $V(x)$ [seen in comparing Figs. 4 and 5(a)] clearly shifts all the eigenvalues of the potential $V(x)$ upwards. Since the lowest eigenvalue in $V(x)$ was $\varepsilon=0$ all eigenvalues in the potential $V(x)+r(x)$ will be positive and therefore *no* stationary solution exists for the diffusion process in Eq. (28).

The Schrodinger equation with potential $V(x)+r(x)$ in Fig. 5(a) cannot be solved analytically, but can be solved approximately. Indeed, on the interval $|x|<x_{\max}$, where $x_{\max}\equiv x(K_{\max})=\arcsin(1/J\sqrt{c_1/c_2})$, we can represent the bar-

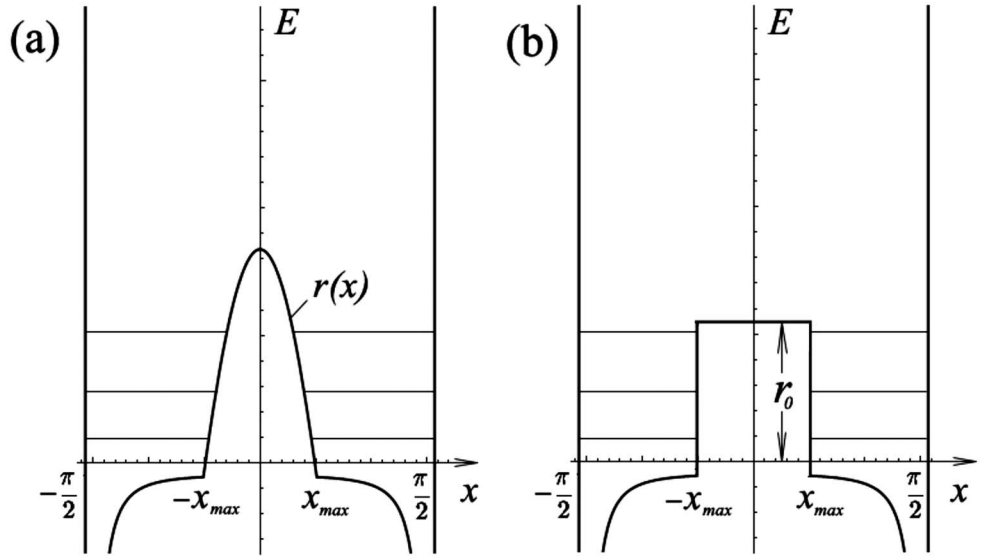

FIG. 5. Effective potential well in Eq. (29). (a) original potential; (b) approximate potential.

rier $r(x)$ with a step function of the average height $r_0 \equiv \int_0^{x_{\max}} r(x)\rho_0(x)dx - D_c/\sqrt{2} = (c_1 - c_2 K_{\max}^2/3) - D_c/\sqrt{2}$, while on the interval $x_{\max} < |x| < \pi/2$ we can approximate $1/\cos^2 x$ with its leading divergent term $1/(|x| - (\pi/2))^2$. The approximate Schrodinger potential is then

$$V^{(0)}(x) = \begin{cases} +\infty, & |x| = \frac{\pi}{2}, \\ -\frac{D_c}{2}\left(1 + \frac{\sqrt{2}-1}{\left(|x| - \frac{\pi}{2}\right)^2}\right), & x_{\max} < |x| < \frac{\pi}{2}, \\ r_0, & |x| < x_{\max}, \end{cases} \tag{30}$$

and is illustrated in Fig. 5(b). For the eigenstates below the barrier r_0, i.e., with the corresponding eigenvalues $\tilde{\varepsilon}_n < r_0$, the potential given by Eq. (30) results in eigenfunctions of the form given in Eq. (31) as shown in Appendix B,

$$\tilde{\psi}_n(x) = \begin{cases} C_1 \sqrt{\frac{\pi}{2}} \sqrt{k\left(\frac{\pi}{2} - |x|\right)} J_q\left[k\left(\frac{\pi}{2} - |x|\right)\right], & x_{\max} < |x| < \frac{\pi}{2}, \\ C_2 \sinh(\kappa x) + C_3 \cosh(\kappa x), & |x| < x_{\max}, \end{cases} \tag{31}$$

where $J_q(x)$ is a Bessel function of the first kind, $q = (\sqrt{2}-1)/2$, $k = \sqrt{(\tilde{\varepsilon}_n/D_c) + (1/2)}$, $\kappa = \sqrt{|r_0 - \tilde{\varepsilon}_n|/D_c}$ and $\tilde{\varepsilon}_n$ is the corresponding eigenvalue. The coefficients C_1, C_2 and C_3 are found from continuity and normalization conditions. For large values of x the asymptotic approximation holds, $J_q(x) \approx \sqrt{2/\pi x}\cos(x - ((q\pi)/2) - (\pi/4))$. Therefore since the minimum value of the expression $k((\pi/2) - x_{\max})$ is approximately π (as seen in the analysis below) we can use the above approximation at the connection points at $|x| = x_{\max}$ to find $\tilde{\varepsilon}_n$ and the corresponding C_1, C_2 and C_3. We thus obtain

$$|C_1| \approx \frac{1}{\sqrt{\frac{\pi}{2} - x_{\max}}}$$

$$C_2 = \begin{cases} 0, & \text{for even states}, \\ \frac{k}{\sqrt{k^2 + \kappa^2}} \frac{C_1}{\sinh(\kappa x_{\max})}, & \text{for odd states}, \end{cases} \tag{32}$$

$$C_3 = \begin{cases} \frac{k}{\sqrt{k^2 + \kappa^2}} \frac{C_1}{\cosh(\kappa x_{\max})}, & \text{for even states}, \\ 0, & \text{for odd states}, \end{cases}$$

and the equation to find $\tilde{\varepsilon}_n$ is

$$\cot\left[k\left(\frac{\pi}{2} - x_{\max}\right) - \frac{\pi q}{2} - \frac{\pi}{4}\right] = \frac{k}{\kappa}. \tag{33}$$

We can find an approximate expression for $\tilde{\varepsilon}_n$ retaining the first-order term in the expansion of $\operatorname{arccot}(x) = \operatorname{arccot}(0) - x$,

$$\tilde{\varepsilon}_n = D_c \left\{ \left[\frac{\pi\left(n + \frac{3}{4} + \frac{q}{2}\right)}{(\pi/2) - x_{\max} + \sqrt{\frac{D_c}{r_0}}} \right]^2 - \frac{1}{2} \right\}. \tag{34}$$

In particular, the lowest eigenvalue is

$$\tilde{\varepsilon}_0 = D_c \left\{ \left[\frac{\pi\left(\frac{3}{4} + \frac{q}{2}\right)}{(\pi/2) - x_{\max} + \sqrt{\frac{D_c}{r_0}}} \right]^2 - \frac{1}{2} \right\}, \tag{35}$$

and, as we show below, determines the long-time decay of the lifetime distribution in Fig. 3.

For the eigenstates with $\tilde{\varepsilon}_n > r_0$ we find by analogy

$$\tilde{\psi}_n(x) = \begin{cases} C_1\sqrt{\frac{\pi}{2}}\sqrt{k\left(\frac{\pi}{2}-x\right)}J_q\left[k\left(\frac{\pi}{2}-x\right)\right], & x_{\max} < |x| < \frac{\pi}{2}. \\ C_2\sin(\kappa x) + C_3\cos(\kappa x), & |x| < x_{\max}, \end{cases} \tag{36}$$

with

$$|C_1| = \left[\frac{\pi}{2} + \frac{(k^2-\kappa^2)x_{\max}}{k^2\cot^2(\kappa x_{\max}) + \kappa^2}\right]^{-1/2},$$

$$C_2 = \begin{cases} 0, & \text{for even states,} \\ \frac{k}{\sqrt{k^2+\kappa^2\cot(\kappa x_{\max})^2}}\frac{C_1}{\sin(\kappa x_{\max})}, & \text{for odd states,} \end{cases} \tag{37}$$

$$C_3 = \begin{cases} \frac{k}{\sqrt{k^2+\kappa^2\tan(\kappa x_{\max})^2}}\frac{C_1}{\cos(\kappa x_{\max})}, & \text{for even states,} \\ 0, & \text{for odd states,} \end{cases}$$

and the equation to determine $\tilde{\varepsilon}_n$ is

$$\tan\left[k\left(\frac{\pi}{2}-x_{\max}\right) - \frac{\pi q}{2} - \frac{\pi}{4}\right] = -\frac{\kappa}{k}\tan(\kappa x_{\max}). \tag{38}$$

C. Analytical expression of the lifetime distribution function

The eigenfunctions $\tilde{\varphi}_n(x)$ and eigenvalues $\tilde{\varepsilon}_n$ of the operator $\tilde{L}_{\mathrm{FP}}$, found in the previous section, allow one to derive an approximate analytical expression for the lifetime distribution function of vibrationally excited ozone molecules. Representing a δ-function in terms of eigenfunctions $\tilde{\varphi}_n(x)$, as in Appendix A, we obtain the following expression for the transition probability $p(x,t|x't')$, see Ref. 6,

$$\begin{aligned} p(x,t|x't') &= e^{\tilde{L}_{\mathrm{FP}}(x)(t-t')}\delta(x-x') \\ &= e^{\Phi(x')}\sum_n e^{\tilde{L}_{\mathrm{FP}}(x)(t-t')}\tilde{\varphi}_n(x)\tilde{\varphi}_n(x') \\ &= e^{\Phi(x')}\sum_n \tilde{\varphi}_n(x)\tilde{\varphi}_n(x')e^{-\tilde{\varepsilon}_n(t-t')} \\ &= e^{\Phi(x')/2-\Phi(x)/2}\sum_n \tilde{\psi}_n(x)\tilde{\psi}_n(x')e^{-\tilde{\varepsilon}_n(t-t')} \end{aligned} \tag{39}$$

where the quantities appearing in Eq. (39) are given by Eqs. (21) and (31)–(37). Given the initial distribution density $\tilde{\rho}_0(x)$ in Eq. (16), the distribution density $\tilde{\rho}(x,t)$ at arbitrary time is

$$\begin{aligned} \tilde{\rho}(x,t) &= \int p(x,t|x'0)\tilde{\rho}_0(x')dx' \\ &= e^{-\Phi(x)/2}\sum_n \tilde{\psi}_n(x)e^{-\tilde{\varepsilon}_n t}\int_{-\pi/2}^{\pi/2}\tilde{\psi}_n(x')e^{\Phi(x')/2}\tilde{\rho}_0(x')dx'. \end{aligned} \tag{40}$$

Clearly, only *even* eigenfunctions $\tilde{\psi}_n(x')$ result in nonzero integral in Eq. (40), since both $\Phi(x')$ and $\tilde{\rho}_0(x')$ are even. The lifetime distribution function $P(t)=\int\tilde{\rho}(x,t)dx$ is then given by

$$\begin{aligned} P(t) = \int_{-\pi/2}^{\pi/2}\tilde{\rho}(x,t)dx &= \sum_n e^{-\tilde{\varepsilon}_n t}\left[\int_{-\pi/2}^{\pi/2}e^{-\Phi(x)/2}\tilde{\psi}_n(x)dx\right] \\ &\times\left[\int_{-\pi/2}^{\pi/2}\tilde{\psi}_n(x')e^{\Phi(x')/2}\tilde{\rho}_0(x')dx'\right] \\ &\equiv P_{\varepsilon<r}(t) + P_{\varepsilon>r}(t), \end{aligned} \tag{41}$$

where we define the sum over those eigenstates that lie below the barrier r_0, i.e., $\tilde{\varepsilon}_n < r_0$, by $P_{\varepsilon<r}(t)$ and the sum of terms with $\tilde{\varepsilon}_n > r_0$ by $P_{\varepsilon>r}(t)$.

For $P_{\varepsilon<r}(t)$, the first integral in Eq. (41) is determined by behavior of $\tilde{\psi}_n(x)$ on the interval $x_{\max} < |x| < \pi/2$ since on the interval $|x| < x_{\max}$ it is exponentially small, as seen in Eq. (31). Yet, on the interval $x_{\max} < |x| < \pi/2$ functions $\tilde{\psi}_n(x)$ oscillate and therefore the first integral in Eq. (41) is significant only for the $\tilde{\psi}_n(x)$ that have even number of nodes, which means that in addition to the requirement of even functions $\tilde{\psi}_n(x)$ only the eigenfunctions with $n=0,2,4,\ldots$ will make dominant contribution. Using Eqs. (21), (31), and (32) we therefore obtain

$$P_{\varepsilon<r}(t) \approx \frac{4D_c}{\left(\frac{\pi}{2}-x_{\max}\right)\sin(x_{\max})}\sum_{n=2k}^{\tilde{\varepsilon}_n<r_0}\frac{1}{\sqrt{r_0(r_0-\tilde{\varepsilon}_n)}}e^{-\tilde{\varepsilon}_n t}, \tag{42}$$

where $\tilde{\varepsilon}_n$ is given by Eq. (34) and r_0 is approximately the average rate $\langle r(x)\rangle$ at a given total energy E and total angular momentum J: $r_0 \equiv \langle r(x)\rangle - D_c/\sqrt{2} = k_r(E - E_{\mathrm{diss}} - (J^2/2\sqrt{\langle I_2\rangle\langle I_3\rangle})) - k_r[(1/2\langle I_1\rangle) - (1/2\sqrt{\langle I_2\rangle\langle I_3\rangle})] \times K_{\max}^2/3 - D_c/\sqrt{2}$, see Eq. (7).

In the derivation of Eq. (42) and further analytical expressions in this section we use several approximations based on physical grounds: we assume $D_c \ll r_0$ which means that rotational-vibrational energy exchange is much slower than the dissociation rate r_0; and we consider $x_{\max}$ such that it is neither too close to its minimum value 0 nor it is too close to its maximum value $\pi/2$. In this way we have competitive contributions of both processes: the process of dissociation and the process of rotational-vibrational energy exchange. (Otherwise for small $x_{\max}$ rotational-vibrational energy exchange dominates dissociation and for $x_{\max}$ close to $\pi/2$ the effect of Coriolis rotational-vibrational energy transfer is small.)

For $P_{\varepsilon>r}(t)$, we note that $\tilde{\psi}_n(x)$ now oscillates everywhere, including the interval $|x| < x_{\max}$, see Eq. (36). Due to the oscillatory nature of $\tilde{\psi}_n(x)$ for $|x| < x_{\max}$, the second integral in Eq. (41) is dominated by those $\tilde{\psi}_n(x)$ that have nodes near $x = \pm x_{\max}$, i.e., $\tilde{\psi}_n(\pm x_{\max}) \approx 0$ (in this case the number of positive and negative half-periods of $\cos(\kappa x)$ differs by one and do not compensate each other in the integral). The

condition $\tilde{\psi}_n(\pm x_{\max}) \approx 0$ means $\cos(\kappa x_{\max}) \approx 0$, the latter gives eigenvalues of the states which are dominant in summation $P_{\varepsilon>r}(t)$:

$$\tilde{\varepsilon}_n{}' = r_0 + D_c\left(\frac{\pi}{x_{\max}}\right)^2\left(n+\frac{1}{2}\right)^2, n=0,1,2,\ldots. \quad (43)$$

Retaining only these states in summation $P_{\varepsilon>r}(t)$, we obtain

$$P_{\varepsilon>r}(t) \approx \sum_n^{\tilde{\varepsilon}_n>r_0} \frac{2D_c}{(\tilde{\varepsilon}_n{}' - r_0)\sin(x_{\max})x_{\max}} e^{-\tilde{\varepsilon}_n t} \quad (44)$$

in derivation of which we used $\cot(\kappa x_{\max})=0$ and $\tilde{\varepsilon}_n{}'/r_0 \approx 1$ for the states right above the barrier r_0. Introducing Eqs. (42) and (44) into Eq. (41) we finally obtain

$$P(t) = \frac{2D_c}{\sin(x_{\max})}\left\{\frac{1}{\left(\frac{\pi}{2}-x_{\max}\right)}\sum_{n=2k}^{\tilde{\varepsilon}_n<r_0}\frac{2}{\sqrt{r_0(r_0-\tilde{\varepsilon}_n)}}e^{-\tilde{\varepsilon}_n t} + \frac{1}{x_{\max}}\sum_n^{\tilde{\varepsilon}_n>r_0}\frac{1}{(\tilde{\varepsilon}_n{}' - r_0)}e^{-\tilde{\varepsilon}_n{}' t}\right\}, \quad (45)$$

where $\tilde{\varepsilon}_n$ and $\tilde{\varepsilon}_n'$ are given by Eqs. (34) and (43). Equation (45) is the central result of the present paper. It gives the survival probability of an energetically activated ozone molecule to remain undissociated by time t, or in other words the probability of an activated ozone molecule to dissociate by time t is $1-P(t)$. One can check that the obvious requirement of $P(0)=1$ is satisfied by analytical result (45). Indeed, substituting expressions (34) and (43) for $\tilde{\varepsilon}_n$ and $\tilde{\varepsilon}_n'$ we get

$$P(0) = \frac{2}{\sin(x_{\max})}\left\{\frac{2D_c}{r_0\left(\frac{\pi}{2}-x_{\max}\right)}\sum_{n=2k}^{\tilde{\varepsilon}_n<r_0}\frac{1}{\sqrt{a-b(n+c)^2}} + \frac{x_{\max}}{\pi^2}\sum_{n=0}^{\infty}\frac{1}{\left(n+\frac{1}{2}\right)^2}\right\}, \quad (46)$$

where $a=1+D_c/2r_0$, $b=(D_c/r_0)[\pi/(\pi/2-x_{\max}+\sqrt{D_c/r_0})]^2$, and $c=3/4+q/2$. The second sum in Eq. (46) can be calculated exactly and equals $\pi^2/2$. The first sum in Eq. (46) can be approximated via the integral over $2dn$ and results in $(2/\sqrt{b})\arctan[\sqrt{b(n+c)^2/(a-b(n+c)^2)}]|_0^{n_{\max}} \approx (2/\sqrt{b})(\pi/2)$ in our regular approximation $D_c \ll r_0$. Expression (46) thus results in

$$P(0) = \frac{2}{\sin(x_{\max})}\left\{4\sqrt{\frac{D_c}{r_0}}\left[1+\sqrt{\frac{D_c}{r_0}}\frac{1}{\left(\frac{\pi}{2}-x_{\max}\right)}\right]+\frac{x_{\max}}{2}\right\} \approx \frac{x_{\max}}{\sin(x_{\max})} \approx 1. \quad (47)$$

From the Eq. (45) several interesting conclusions can be drawn. First, we notice that the coefficients $1/\sqrt{r_0-\tilde{\varepsilon}_n}$ and $1/(\tilde{\varepsilon}_n - r_0)$ in Eq. (45) make an exponential term with $\tilde{\varepsilon}_n \approx r_0$ dominant at initial times. This result means that at initial times the lifetime statistics is governed by the purely vibrational dissociation rate r_0 as if there were no rotations of ozone molecules at all. The effects of rotations slowly comes in at later times and becomes dominant at long times resulting in the decay rate $\tilde{\varepsilon}_0$, given by the expression (35). One can see from Eq. (35) that exponent $\tilde{\varepsilon}_0$ is directly proportional to the Coriolis coupling parameter D_c and thus, clearly, it is the slow diffusive vibrational-rotational energy exchange that determines long-time behavior of the self-dissociation lifetime statistics.

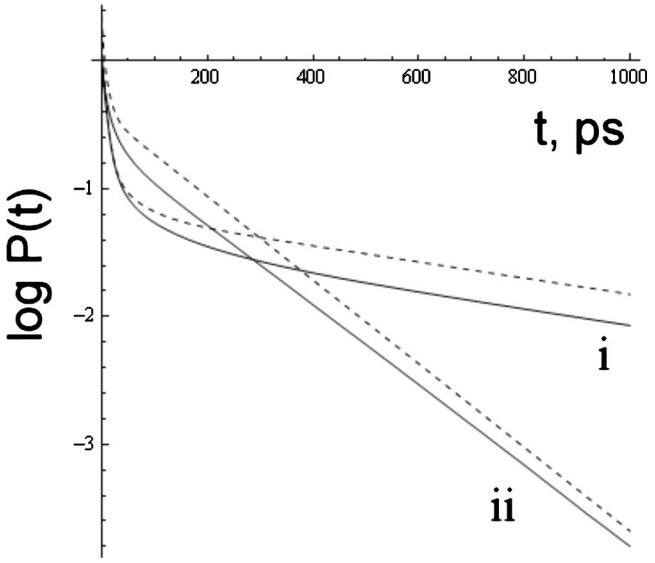

FIG. 6. Comparison of exact and analytical (45) results for potential (30) shown in Fig. 5(b). Solid lines stand for $P(t)$ obtained using exact eigenfunctions of the model (30). Dashed lines represent the approximate analytical expression (45). Curves (i) represent results for the total energy $E=E_{\text{diss}}+kT$, $J=20\hbar$, $D_c=0.0005$ ps^{-1}, and $r_0=0.125$ ps^{-1}; curves (ii) represent results for the total energy $E=E_{\text{diss}}+kT$, $J=20\hbar$, $D_c=0.003$ ps^{-1} and $r_0=0.125$ ps^{-1}.

The analytical expression (45) agrees with the exact nu-

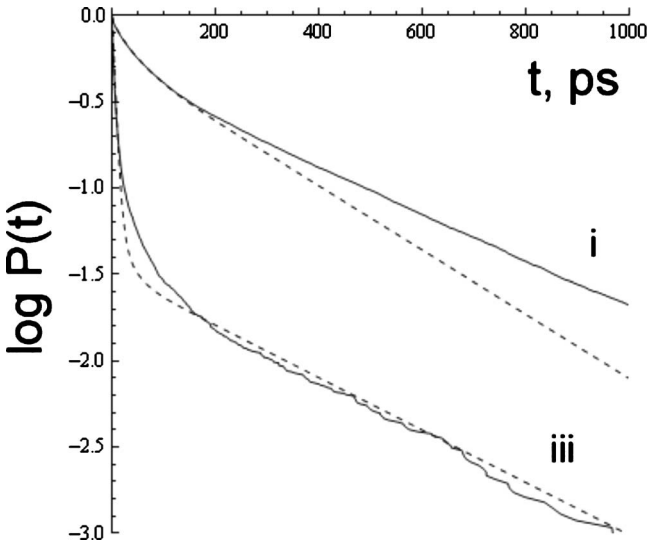

FIG. 7. Comparison between analytical results from Eq. (45) and numerical results of MD simulations from Refs. 3 and 4. The notations used are the same as in Fig. 3. Constant parameter D_c was taken as $D_c(E_{\text{vib}}(J))$. (In case (i) the analytical result (45) is normalized by $P(0)$ and plotted as $P(t)/P(0)$ since in this case the approximation $D_c \ll r_0$ that is necessary for Eq. (45) is not well satisfied).

merical simulation of the model (30), shown in Fig. 6, and describes well the results of the full three-dimensional MD simulations in Refs. 3 and 4, as seen in Fig. 7.

VI. DISCUSSION

In the present paper, we have shown that the non-RRKM effects observed in the lifetime statistics of the vibrationally excited ozone molecules in Refs. 3 and 4 are the result of the diffusive energy exchange between the vibrational and rotational degrees of freedom. If the total energy E and the total angular momentum J are such that $K_{\max}<J$, the K-component of $\mathbf{J}$ may diffuse into the region $|K|>K_{\max}$ where the total vibrational energy of ozone molecule $E_{\mathrm{vib}}=E-E_{\mathrm{rot}}$ is less than the dissociation energy E_{diss}. Once K has diffused to this region, the ozone molecule cannot dissociate and waits until K diffuses back to the region $K<|K_{\max}|$ where dissociation is allowed, as seen in Fig. 1. Therefore, at long times the statistics of ozone self-dissociation lifetimes is governed by the rate of diffusion of K as shown by the analytical expression in Eq. (35). As discussed in Part I, the interval between the molecular collisions at the relevant (atmospheric) pressure conditions of real experiments is long enough for the observed diffusive energy exchange to take place and thus to result in the non-RRKM behavior of ozone dissociation.

We have also derived an approximate analytical expression for the lifetime distribution functions $P(t)$. It follows from the analytical expression, that the rate of decay of $P(t)$ at initial times is governed by the rate of dissociation $r(K)$, i.e., the rate of dissociation which does not include rotational degrees of freedom, while at longer times the effect of Coriolis diffusion becomes dominant and $P(t)$ decays as $\tilde{\varepsilon}_0$, given by Eq. (35), which is proportional to the Coriolis coupling strength D_c.

In cases when the values of the total energy E and rotational angular momentum J do not allow $K_{\max}<J$, i.e., all possible values of K result in vibrational energies that lie above the barrier of dissociation E_{diss}, the diffusive regime is not reachable and the rate of decay of $P(t)$ is governed mostly by the dissociation rate $r(K)$. The latter result provides the reason why some curves $P(t)$ in Refs. 3 and 4 have slow long-time tails while others are "tailless."

APPENDIX A: PROPERTIES OF $\tilde{L}$ OPERATOR

In this appendix, we discuss the properties of operator $\tilde{\boldsymbol{L}}\equiv\exp(\Phi(x)/2)\tilde{\boldsymbol{L}}_{\mathrm{FP}}\exp(-\Phi(x)/2)$, where $\tilde{\boldsymbol{L}}_{\mathrm{FP}}=\boldsymbol{L}_{\mathrm{FP}}-r(x)=D_c(\partial/(\partial x))(\Phi'(x)+(\partial/(\partial x)))-r(x)=D_c(\partial/(\partial x))\exp(-\Phi(x))(\partial/(\partial x))\exp(\Phi(x))-r(x)$ and $\Phi(x)$ given by Eq. (21). Only the case of interest, $x(K_{\max})<x(J)$, is considered. Our derivations follow those in Ref. 6.

(a) $\tilde{\boldsymbol{L}}$ is Hermitian. For any two functions $W_1(x)$ and $W_2(x)$ satisfying zero flux condition $(\Phi'(x)+(\partial/(\partial x)))W=0$ at $x=\pm\pi/2$ we have

$$\begin{aligned}\int_{-\pi/2}^{\pi/2} W_1\tilde{\boldsymbol{L}}W_2dx &= \int_{-\pi/2}^{\pi/2} W_1e^{\Phi(x)/2}\left(D_c\frac{\partial}{\partial x}e^{-\Phi(x)}\frac{\partial}{\partial x}e^{\Phi(x)}-r(x)\right)e^{-\Phi(x)/2}W_2dx\\ &= D_c\int_{-\pi/2}^{\pi/2} W_1e^{\Phi(x)/2}\frac{\partial}{\partial x}\left[e^{-\Phi(x)}\frac{\partial}{\partial x}e^{\Phi(x)/2}W_2\right]dx-\int_{-\pi/2}^{\pi/2} W_2r(x)W_1dx\\ &= -D_c\int_{-\pi/2}^{\pi/2}\left[\frac{\partial}{\partial x}W_1e^{\Phi(x)/2}\right]e^{-\Phi(x)}\left[\frac{\partial}{\partial x}e^{\Phi(x)/2}W_2\right]dx-\int_{-\pi/2}^{\pi/2} W_2r(x)W_1dx\\ &= D_c\int_{-\pi/2}^{\pi/2} W_2e^{\Phi(x)/2}\frac{\partial}{\partial x}e^{-\Phi(x)}\frac{\partial}{\partial x}e^{\Phi(x)}e^{-\Phi(x)/2}W_1dx-\int_{-\pi/2}^{\pi/2} W_2r(x)W_1dx\\ &= \int_{-\pi/2}^{\pi/2} W_2e^{\Phi(x)/2}\left(D_c\frac{\partial}{\partial x}e^{-\Phi(x)}\frac{\partial}{\partial x}e^{\Phi(x)}-r(x)\right)e^{-\Phi(x)/2}W_1dx=\int_{-\pi/2}^{\pi/2} W_2\tilde{\boldsymbol{L}}W_1dx,\end{aligned}\tag{A1}$$

where we have used integration by parts twice along with zero-flux boundary conditions.

(b) If $\tilde{\varphi}_n(x)$ are the eigenfunctions of $\tilde{\boldsymbol{L}}_{\mathrm{FP}}$ with the eigenvalues $\tilde{\varepsilon}_n$ then $\tilde{\psi}_n(x)=\exp(\Phi(x)/2)\tilde{\varphi}_n(x)$ are eigenfunctions of $\tilde{\boldsymbol{L}}$ with the same eigenvalues $\tilde{\varepsilon}_n$
Indeed

$$\tilde{\boldsymbol{L}}(e^{\Phi(x)/2}\tilde{\varphi}_n(x))=e^{\Phi(x)/2}\tilde{\boldsymbol{L}}_{\mathrm{FP}}\tilde{\varphi}_n(x)=e^{\Phi(x)/2}(-\tilde{\varepsilon}_n\tilde{\varphi}_n(x))=-\tilde{\varepsilon}_n(e^{\Phi(x)/2}\tilde{\varphi}_n(x)).\tag{A2}$$

(c) Completeness relations: Since $\tilde{\boldsymbol{L}}$ is Hermitian, its eigenfunctions form a complete basis set, therefore

$$\delta(x-x')=\sum_n\tilde{\psi}_n(x)\tilde{\psi}_n(x')=e^{\Phi(x')}\sum_n\tilde{\varphi}_n(x)\tilde{\varphi}_n(x').\tag{A3}$$

APPENDIX B: SCHRODINGER EQUATION WITH POTENTIAL IN EQ. (30)

In this appendix, we solve stationary Schrodinger equation $-D_c(\partial^2/(\partial x)^2)\psi+V(x)\psi=\varepsilon\psi$ in the potential (30)

$$V(x)=\begin{cases}+\infty, & |x|=\dfrac{\pi}{2},\\ -\dfrac{D_c}{2}\left(1+\dfrac{\sqrt{2}-1}{\left(|x|-\dfrac{\pi}{2}\right)^2}\right), & x_{\max}<|x|<\dfrac{\pi}{2},\\ r_0, & |x|<x_{\max},\end{cases} \tag{B1}$$

For $|x|<x_{\max}$, the solution for ψ is trivial

$$\psi(x)=C_1\cos\left(\sqrt{\frac{\varepsilon-r_0}{D_c}}x\right)+C_2\sin\left(\sqrt{\frac{\varepsilon-r_0}{D_c}}x\right). \tag{B2}$$

For $x_{\max}<x<\pi/2$ the Schrodinger equation reads

$$\frac{\partial^2}{\partial x^2}\psi+\left[\left(\frac{1}{2}+\frac{\varepsilon}{D_c}\right)+\frac{\sqrt{2}-1}{2}\frac{1}{\left(x-\dfrac{\pi}{2}\right)^2}\right]\psi=0. \tag{B3}$$

After substitution $z=\pi/2-x$ Eq. (B3) takes the form of the transformed Bessel equation

$$z^2\frac{d^2\psi}{dz^2}+(2p+1)z\frac{d\psi}{dz}+(\alpha^2z^{2r}+\beta^2)\psi=0. \tag{B4}$$

with $p=-1/2$, $\alpha^2=(1/2+\varepsilon/D_c)$, $r=1$ and $\beta^2=(\sqrt{2}-1)/2$. The solution of Bessel Eq. (B4) is

$$\psi(z)=z^{-p}\left[C_1J_{q/r}\left(\frac{\alpha}{r}z^r\right)+C_2Y_{q/r}\left(\frac{\alpha}{r}z^r\right)\right], \tag{B5}$$

where $J_n(z)$ and $Y_n(z)$ are the Bessel functions of the first and second kinds, respectively, and $q=\sqrt{p^2-\beta^2}=(\sqrt{2}-1)/2$ in our case. The solution of the original Eq. (B3) is therefore

$$\psi(x)=\sqrt{\frac{\pi}{2}-x}\left\{C_1J_q\left(\sqrt{\frac{1}{2}+\frac{\varepsilon}{D_c}}\left(\frac{\pi}{2}-x\right)\right)+C_2Y_q\left(\sqrt{\frac{1}{2}+\frac{\varepsilon}{D_c}}\left(\frac{\pi}{2}-x\right)\right)\right\}. \tag{B6}$$

We now recall the necessary boundary condition (27) for $\psi(x)$: near $x=\pi/2\psi(x)$ should behave as $((\pi/2)-x)^{1/\sqrt{2}}$. Using the lowest order terms of Taylor expansion of the Bessel functions of small argument, i.e., $J_q(x)\sim x^q$ and $Y_q(x)\sim x^{-q}$ we find that the solution (B6) near $x=\pi/2$ behaves as

$$\lim_{x\to\pi/2}\psi(x)\sim C_1\left(\frac{\pi}{2}-x\right)^{1/\sqrt{2}}+C_2\left(\frac{\pi}{2}-x\right)^{1-(1/\sqrt{2})}, \tag{B7}$$

obviously we should have $C_2=0$ to satisfy the boundary condition mentioned above. This means that only the Bessel function of the first kind satisfy boundary conditions (27), and thus for $\psi(x)$ on the interval $x_{\max}<x<\pi/2$ we finally have

$$\psi(x)=C_1\sqrt{\frac{\pi}{2}-x}J_q\left(\sqrt{\frac{1}{2}+\frac{\varepsilon}{D_c}}\left(\frac{\pi}{2}-x\right)\right). \tag{B8}$$

The solution on the interval $-\pi/2<x<-x_{\max}$ can be found by analogy

$$\psi(x)=C_1'\sqrt{\frac{\pi}{2}+x}J_q\left(\sqrt{\frac{1}{2}+\frac{\varepsilon}{D_c}}\left(\frac{\pi}{2}+x\right)\right). \tag{B9}$$

[1] M. Kryvohuz and R. A. Marcus, J. Chem. Phys. **132**, 224304 (2010).
[2] M. V. Ivanov, S. Y. Grebenshchikov, and R. Schinke, J. Chem. Phys. **120**, 10015 (2004).
[3] N. Ghaderi and R. A. Marcus (to be submitted).
[4] N. Ghaderi and R. A. Marcus (to be submitted).
[5] Y. Q. Gao and R. A. Marcus, J. Chem. Phys. **116**, 137 (2002).
[6] H. Risken, *The Fokker-Planck Equation: Methods of Solution* (Springer-Verlag, Tokyo, 1989).
[7] H. W. Schranz, S. Nordholm, and G. Nyman, J. Chem. Phys. **94**, 1487 (1991).
[8] C. W. Gardiner, *Handbook of Stochastic Methods for Physics, Chemistry and the Natural Sciences* (Springer-Verlag, Heidelberg, 2004).
[9] D. L. Bunker and W. L. Hase, J. Chem. Phys. **59**, 4621 (1973).